

1 ChIP-AP – An Integrated ChIP-Seq Analysis Pipeline

2

3 **Jeremiah Suryatenggara¹, Kol Jia Yong^{1,2}, Danielle E. Tenen³, Daniel G. Tenen^{1,4}, Mahmoud A.**
4 **Bassal^{1,4}**

5 1 – Cancer Science Institute of Singapore, National University of Singapore, Singapore

6 2 – Department of Biochemistry, Yong Loo Lin School of Medicine, National University of
7 Singapore, Singapore

8 3 – Broad Institute of MIT and Harvard, Boston, Massachusetts, USA

9 4 – Harvard Stem Cell Institute, Boston, Massachusetts, USA

10

11 **Correspondence:**

12 daniel.tenen@nus.edu.sg

13 mahmoud.bassal@mymail.unisa.edu.au

14

15 **Abstract**

16 ChIP-Seq is a technique used to analyse protein-DNA interactions. The protein-DNA complex is
17 pulled down using a protein antibody, after which sequencing and analysis of the bound DNA
18 fragments is performed. A key bioinformatics analysis step is “peak” calling - identifying regions of
19 enrichment. Benchmarking studies have consistently shown that no optimal peak caller exists. Peak
20 callers have distinct selectivity and specificity characteristics which are often not additive and seldom
21 completely overlap in many scenarios. In the absence of a universal peak caller, we rationalized one
22 ought to utilize multiple peak-callers to 1) gauge peak confidence as determined through detection by
23 multiple algorithms, and 2) more thoroughly survey the protein-bound landscape by capturing peaks
24 not detected by individual peak callers owing to algorithmic limitations and biases. We therefore
25 developed an integrated ChIP-Seq Analysis Pipeline (ChIP-AP) which performs all analysis steps
26 from raw fastq files to final result, and utilizes four commonly used peak callers to more thoroughly
27 and comprehensively analyse datasets. Results are integrated and presented in a single file enabling
28 users to apply selectivity and sensitivity thresholds to select the consensus peak set, the union peak
29 set, or any sub-set in-between to more confidently and comprehensively explore the protein-bound
30 landscape. (<https://github.com/JSuryatenggara/ChIP-AP>).

31 Introduction

32 ChIP-Seq is an extensively used experimental technique that aims to identify DNA binding location
33 sequences and motifs of DNA-interacting proteins such as transcription factors^{1,2}, histone-modifier
34 proteins³, or novel DNA-binding proteins. To perform a ChIP-Seq experiment, cells are fixed, the
35 chromatin-protein complex sonicated, and the DNA fragments interacting with the protein of interest
36 pulled down by the targeted protein antibody. Following experimental pull-down of the
37 protein-bound DNA and sequencing, the raw sequencing data (raw fastq files) undergoes processing
38 and analysis, after which, biological relevance can be inferred⁴. Such analyses, in conjunction with
39 follow up mechanistic studies, shed light on the DNA-associated proteins biological function and
40 roles⁴.

41

42 Since the development of ChIP-Seq^{2,5,6}, computational analysis of ChIP-Seq experiments has always
43 been a multi-step process requiring multiple command line programs which, to use most effectively,
44 requires knowledge and experience in computing and programming⁴. Wet-lab biologists without
45 command line or coding experience have typically relied on bioinformaticians, with their computing
46 expertise, to analyse the sequenced data despite them potentially having a reduced understanding of
47 the underlying biology. Irrespective of whom performs the analysis however, in the computational
48 space, many analogous programs have been developed for each stage of the analysis, complicating
49 how one should approach an analysis and the decision of which programs to use in conjunction with
50 one-another. It is therefore easy to understand why two different analysis methodologies, even if they
51 appear superficially identical or similar, will almost certainly report different results, leading to
52 conflicting conclusions from the same biological experiment^{7,8}. To complicate matters further,
53 published methods outlining the workflow used to analyse a dataset will consistently lack essential
54 details, with some authors omitting key program modification parameters/flags, or neglecting to
55 include key analysis steps entirely, relegating published analyses to being almost entirely
56 irreproducible for other researchers.

57

58 Of all the complications plaguing ChIP-Seq analyses though, perhaps the most well-known source of
59 inconsistency between analyses is the choice of peak calling algorithm^{2,7,8}. This observation was
60 convincingly demonstrated by Steinhauser et. al.⁸ in their study comparing 20 peak callers wherein
61 they reported poor agreement between the called peak sets across the profiled callers. This, and other
62 studies, therefore show that peak callers have distinct selectivity and specificity characteristics which
63 are often not additive and seldom completely overlap in many scenarios⁸⁻¹¹. Consequently, such
64 differing operating characteristics results in a lack of consistency across the reported regions of
65 enrichment (and associated genes) for each peak caller. This has follow-on effects in that
66 downstream functional analysis for the protein of interest would therefore give differing, potentially
67 conflicting results. Additionally, it has been shown extensively that the performance of a peak caller
68 is subject to the read characteristics and read distributions of the dataset in question⁸⁻¹². An individual
69 peak caller can outperform other callers in certain datasets but will perform poorly in alternate
70 datasets. Therefore, relying on a one-caller-fits-all approach when analysing datasets with different
71 DNA-binding proteins, immunoprecipitation and library preparation protocols is objectively not the
72 soundest approach to yield reliable, consistent and comprehensive results.

73

74 We therefore rationalized that in order to improve the reliability and consistency of a ChIP-Seq
75 analysis, one ought to focus on and improve the consistency, confidence and comprehensiveness of
76 the peak detection step without requiring additional wet-lab observations. To address this, we
77 designed our ChIP-Seq Analysis Pipeline (ChIP-AP) which integrates all processes of a ChIP-Seq
78 analysis (from raw fastq to final result) into a single, easy to use package, that utilizes four
79 commonly used peak callers¹³⁻¹⁷ (for either transcription factors or histone modifier proteins), and
80 integrates their results into a single output file, from which, users are able to infer peak confidence. If
81 a peak is called by multiple callers, one can infer that the reported peak has a higher confidence and
82 is less likely to be a false-positive or an artefact of algorithmic bias or limitation. Alternatively, by
83 integrating the results of all the callers (the union of all peaks), one can more comprehensively
84 survey the binding landscape of the binding protein by capturing peaks that would otherwise be
85 uncalled or “lost” if relying on a lone peak caller. In other words, the union peak set enables a more

86 comprehensive survey of the binding landscape by accepting all peaks irrespective of confidence. By
87 utilizing multiple peak callers and integrating their results, users are able to determine the selectivity
88 and specificity requirements that best describe their dataset while allowing them to circumvent
89 inherent sample characteristics that result in poor peak calling performance of any single peak caller,
90 thus enabling the capture of either the most number of peaks (the union of all peaks), the most
91 confident peaks (the consensus results), or any sub-set of the gradient in-between. ChIP-AP can
92 therefore become an effective tool for users by providing both substantial improvements to peak
93 capturing and analysis reliability. ChIP-AP is available on GitHub
94 (<https://github.com/JSuryatenggara/ChIP-AP>) with extensively detailed wiki pages describing
95 installation, use and results interpretation (<https://github.com/JSuryatenggara/ChIP-AP/wiki>).

96

97 Results

98 Consensus peaks increase motif and ontology accuracy

99 A reproducible result instils greater confidence in its validity. Likewise, ChIP-Seq peaks that can be
100 detected by multiple peak callers, each utilizing different peak detection algorithms, garner greater
101 confidence than peaks called by an individual peak caller. ChIP-AP, with its utilization of four
102 different peak callers, reports along-side the coordinates of a peak how many callers detected the said
103 peak. Using this, users are able to filter on the consensus peaks, which are the peaks detected by all
104 four peak callers and, consequently, carry the greatest confidence. We hypothesized that utilizing the
105 consensus peak set would increase the percentage of peaks containing a valid binding motif
106 (peak-motif percentage) without drastically affecting the motif position bias (the distance of the motif
107 to the weighted peak center). The consensus peak set would also increase the likelihood of identifying
108 correct binding motifs while masking co-factor binding artifacts. Finally, the consensus peak set
109 should also improve gene ontology (GO) results by ensuring only the strongest binding candidates are
110 included in analysis.

111

112 To investigate whether the peak-motif percentage for the consensus peak set is significantly better
113 than using a single peak caller (MACS2), we processed 10 transcription factor (TF) datasets from

114 differing TF families, across 3 cell lines sourced from ENCODE¹⁸, and determined their peak-motif
115 percentage (see **Methods** for sample details). For each TF, we downloaded the binding motif from
116 MethMotif¹⁹ (which sourced its motifs from JASPAR 2018²⁰), and determined how many peaks
117 contain the binding motif while allowing up to a single sequence mismatch. As expected, a significant
118 difference in the average peak-motif percentage was observed across all 10 TF's (two-tailed t-test
119 $p=0.0012$, **Figure 1a**). The degree by which the consensus peak set improved the peak-motif
120 percentage was variable, with an up to 90% improvement for RUNX1, but none the less, still showed
121 improvement for all 10 TFs over the MACS2 peak set alone (**Supplemental Table 1**).

122

123 We next investigated whether the consensus peak set significantly altered the motif position bias with
124 respect to the weighted peak center as compared to individual callers. Across all 10 TFs, the benefit of
125 the consensus peak set was variable, with it out-performing all individual peak callers in some
126 datasets (**Figure 1b, Supplemental Table 2**), while in others, providing comparable results
127 (**Supplemental Figure 1a, Supplemental Table 2**). Consistently though, the consensus peak set did
128 show significant improvement over at least half the peak callers tested suggesting that utilizing the
129 consensus peak set will either give an improved motif position bias profile or report comparable
130 results to having used an individual peak caller.

131

132 Next, we questioned whether the consensus peak set can provide improved *de novo* motif sequence
133 detection while masking co-factor binding artefacts. Previously, Lin et al.²¹ described that *de novo*
134 global motif analyses can potentially be contaminated by co-factor motif sequence artefacts. In their
135 publication, they highlighted potential co-factor motif artefacts for CEBPB and MAFF. Using
136 ChIP-AP, we performed *de novo* motif analysis using HOMER¹⁵ and the MEME-Suite²²⁻²⁴ for the
137 MACS2 called and the consensus peak set for these two TFs. For CEBPB, the first candidate motif hit
138 reported by HOMER for both the consensus and the MACS2 peak sets was near identical, which,
139 according to Lin et al.²¹, contains co-factor binding motif artefacts (**Figure 1c, d** upper panels).

140 However, the second motif hit for the consensus peak set (**Figure 1c** lower panel) shows the clean
141 binding motif sequence TTGC, which is the CEBPB motif that contains neither co-factor motif
142 contamination nor a heterodimer sequence²¹. The MACS2 peak set's second motif result however
143 (**Figure 1d**, lower panel), failed to report the same motif result. When analysed using the
144 MEME-Suite, the consensus peak set showed two motifs with co-factor artefacts (**Supplemental**
145 **Figure 1b**, 1st and 3rd ranked), two motifs with the heterodimer sequence (**Supplemental Figure 1b**,
146 2nd and 4th ranked) and the fifth result showed the TTGC binding motif without co-factor motif
147 contamination nor a heterodimer sequence. Conversely, for the MACS2 dataset as analysed by the
148 MEME-Suite, three motif results contain co-factor sequence artefacts (**Supplemental Figure 1c**, 1st,
149 3rd and 4th ranked), one result with heterodimer sequence (**Supplemental Figure 1c**, 2nd ranked) and
150 the fifth result was also the TTGC binding motif without co-factor motif contamination nor a
151 heterodimer sequence. Therefore, for CEBPB, although both *de novo* motif algorithms reported
152 similar findings, the consensus peak set showed a cleaner and more direct signal for the CEBPB
153 binding motif from the second HOMER result, a finding not immediately evident in the MACS2 set
154 without careful inspection of the data.

155

156 For the TF MAFF, the HOMER *de novo* motif result for the consensus peak set remained more
157 consistent (**Figure 1e**) with both the top two motif results showing the binding sequence TCAGCA.
158 The MACS2 peak set however, wasn't as consistent showing different sequences between the first
159 and second motif candidates (**Figure 1f**). Similarly for the MEME-Suite results (**Supplemental**
160 **Figure 1d, e**), MEME consistently calls the TGCTGA for both peak sets but the 6th reported motif
161 candidate for the consensus peak set shows a heterodimer binding profile (characterised by the
162 "sequence - spacer - reverse complement sequence" profile), a result not recapitulated in the MACS2
163 peak set entirely, thereby supporting the notion that the consensus peak set can provide more direct
164 *de novo* enriched motif results over using a single peak caller alone.

165

166 Our final investigation was to test whether the consensus peak set can provide improved, more direct
167 gene ontology (GO) results. In running a GO analysis for all 10 TF's profiled and comparing the
168 consensus peak set results to the MACS2 peak sets, we observed that for certain datasets, such as
169 RUNX1, ATF4, JUN, ZBTB33 and GATA1, the consensus peak set GO results returned more
170 relevant and directly related terms than the MACS2 peak set (**Table 1, Supplemental Tables 3, 4**).
171 For the RUNX1 results, whereas the top 20 MACS2 GO results contained generic GO terms, the
172 consensus peak GO listing clearly outlined RUNX1 functions regarding hematopoietic differentiation,
173 regulation of metabolic and signalling pathways and autophagy regulation, all of which are known
174 published functions of RUNX1²⁵⁻³⁰ (**Table 1**). The GO terms returned when searching the consensus
175 peak candidate list can therefore, for certain datasets, provide significantly clearer and more direct GO
176 results by providing information on only the gene terms corresponding to the most confident peaks
177 called by all peak callers.

178

179 Therefore, utilizing the consensus peak set can provide added benefits to identify novel binding motifs
180 or to identify more direct biological processes modulated by a protein of interest, especially if it is not
181 well characterized as evidenced by the results presented. In all metrics investigated, the consensus
182 peak set's performance was either significantly improved, or, in worst performing cases, provided
183 results comparable to having used only a single peak caller.

184

185 **Capturing Lost Peaks with the Union Peak Set**

186 A number of variables can affect a ChIP-Seq experiments efficiency resulting in poor enrichment and
187 potentially giving rise to a high signal:noise ratio dataset. Every peak caller has differing operating
188 characteristics and thus, has differing abilities to handle these difficult to process datasets^{8,12}. A
189 ChIP-Seq analysis utilizing only a single peak caller would be solely dependent on the chosen peak
190 callers' ability to handle the signal:noise ratio and enrichment characteristics of that dataset. If the
191 peak caller struggles to differentiate signal from noise effectively, few peaks will be called and a
192 dataset will give an inconclusive result owing to its ineffectiveness to deal with the dataset. However,

193 some peak callers are more capable at handling difficult datasets, and so an experiment may show
194 poor enrichment, but it simply needs to be analysed with the right peak caller for its specific
195 characteristics, the choice of which may not be evident or obvious in advance.

196

197 One protein that is relatively difficult to perform ChIP-Seq on, is the oncogene sal-like protein 4
198 (SALL4). SALL4 has been shown to play essential roles in maintaining pluripotency and self-renewal
199 characteristics of embryonic stem cells (ESC)³¹. It is typically down-regulated after birth but has been
200 found to be aberrantly regulated in many tumors^{31,32}. Studies have also shown SALL4 to have
201 multiple protein interacting partners and DNA-binding and regulation functions^{31,33}. An attempt to
202 capture the DNA-binding partners of SALL4 was undertaken with the sequenced result showing poor
203 enrichment on the fingerprint plot with little separation between the SALL4 ChIP-Seq replicate and
204 control curves (**Figure 2a**), indicating it will likely be difficult to call peaks for this dataset. When
205 processed with ChIP-AP, we observed that peak callers GEM and MACS2 struggle to call peaks
206 (**Figure 2b**) with each returning a total of 1,362 and 1,937 peaks respectively. HOMER, is able to call
207 approximately double the number of peaks at 3,760. However, Genrich, which determines peaks using
208 an area under the curve (AUC) calculation rather than generating a Poisson distribution model (as
209 seen in MACS2, GEM and HOMER), is more successful in dealing with such a dataset and calls a
210 total of 12,452 peaks. We therefore sought to investigate the efficacy of utilizing the union peak set
211 for this poorly enriched SALL4 ChIP-Seq, which enables us to sacrifice specificity for a gain in
212 sensitivity across the dataset, ie, we accept all peaks including those called by only a single peak
213 caller which carry less confidence but provide higher sensitivity (**Supplemental Table 5**).

214

215 To test its validity, we compared the SALL4 ChIP-Seq union peak set with a SALL4 Cut&Run
216 dataset recently published³³. Cut&Run is a technique which utilizes antibody-targeting and
217 micrococcal nuclease digestion to map global DNA binding sites³⁴. It is an analogous but independent
218 technique to ChIP-Seq thus providing an independent dataset for comparison and validation. To

219 ensure the peaks called in our ChIP-Seq were likely binding targets of SALL4, we first directly
220 compared the union peak set to the SALL4 Cut&Run dataset. Reassuringly, the union peak set
221 showed a 36% overlap with peaks identified in at least 2 of the Cut&Run replicates (3 biological
222 replicates total) (**Figure 2c**). Using individual peak callers, overlap percentages ranging from 25-56%
223 were observed with fewer peaks called (**Supplemental Figure 2a**). Furthermore, each caller reports a
224 different sub-set of targets with little overlap between them (**Figure 2b**). However, by considering the
225 union peak set, we can gain a more complete overview of the binding landscape without significantly
226 affecting average sensitivity, by allowing us to circumvent the poor performance of individual peak
227 callers for the dataset in question and call “missed” peaks.

228

229 Next, we wanted to confirm that the called union peaks show our recently identified human SALL4
230 DNA binding motif³³. To investigate this, we performed a directed motif search wherein we searched
231 every peak in the union peak set for the human SALL4 DNA binding motif. This showed that 55% of
232 the union peak set contained at least one instance of our identified SALL4 motif (**Figure 2d**), a result
233 comparable to using an individual peak caller alone (**Supplemental Table 1, 6**). To ensure we have
234 not biased the motif search, we performed a *de novo* motif search on the union peak set using both the
235 MEME-Suite²²⁻²⁴ (which utilize the algorithms STREME, CentriMo and MEME-ChIP) and HOMER
236 which were both able to call the human SALL4 DNA binding motif as the second and third top
237 candidate motif hits respectively (**Figure 2e, f**). According to CentriMo, the STREME identified
238 motif is centrally enriched in individual peaks in the union peak set (**Figure 2g**), an expected
239 observation for true binding motif sequences. Furthermore, MEME-ChIP itself, called the same motif
240 as the third candidate peak with the second candidate motif result also being an AT rich motif with
241 near identical sequence (**Supplemental Figure 2b**). We therefore concluded that despite the
242 additional number of peaks called by taking the union peak set, the SALL4 DNA-binding motif
243 signature is still present across all called peaks and is identifiable using multiple algorithms as a top
244 three candidate motif.

245

246 As further validation to ensure the union peak set identified valid targets of SALL4, a GO analysis
247 was performed and compared with the results of previous findings³³. We previously reported that
248 SALL4 knock-down resulted in a significant increase in the number of up-regulated genes in the
249 “*transcriptional regulator activity*” (GO:0140110) pathway, results which were validated by
250 comparing bulk RNA-Seq and Cut&Run results³³, and thus confirming pathway members as *bona fide*
251 SALL4 targets. Consistently, the GO analysis on the union peak set identified the same pathway as a
252 top 20 enriched pathway (**Supplemental Table 7**), with more significantly enriched terms pointing to
253 SALL4 being a DNA-binding protein; a well-established function of SALL4^{31,32} (**Supplemental**
254 **Table 7**). Therefore, despite utilizing the union peak set which sacrificed a degree of specificity, the
255 peak set was still valid in detecting accurate biological functions of SALL4.

256

257 The final validation to ensure the union dataset identified valid targets of SALL4 was to overlap the
258 union peaks gene list with the SALL4 knock-down bulk RNA-Seq previously published³³, and
259 compare the overlap targets of the union peak set with the overlapping targets of the Cut&Run
260 dataset. We previously reported that 2,695 genes were found significantly differentially expressed on
261 SALL4 knock-down, 430 of which has a corresponding annotated SALL4 Cut&Run peak. Using the
262 union peak set, we observed an overlap of 451 genes (**Supplemental Table 8**) with the SALL4
263 knock-down dataset, of which, 198 gene targets were found in common between the Cut&Run and
264 ChIP-Seq gene sets (**Supplemental Table 8**). This finding combined with the observed overlap
265 between the union peak set and the Cut&Run replicates suggests that there are SALL4 binding targets
266 that were detected by the ChIP-Seq that were not detected by the Cut&Run and vice versa. However,
267 both the Cut&Run and the union peak list derived from the SALL4 ChIP-Seq appear to still be calling
268 valid SALL4 target genes with significant overlaps between the two datasets observed.

269

270 Taken together, the results obtained show that despite this SALL4 ChIP-Seq showing poor
271 enrichment with few peaks called by two of the four peak callers, there was still valid data within the

272 dataset that can be extracted, used, and validated by independent approaches³³. By considering the
273 union peak set generated by ChIP-AP, one can opt to marginally sacrifice specificity for a significant
274 gain in sensitivity across the dataset and confirm the presence of peaks identified or validated using
275 different methodologies should the characteristics of the dataset prove to be less than favourable.
276 Whereas previous analyses using a single peak caller would produce sub-optimal results, by relying
277 on multiple peak callers, as ChIP-AP does, sub-optimal datasets can be salvaged and still report valid
278 findings.

279

280 ChIP-AP Functionality and Characteristics

281 ChIP-AP Modularity for Advanced Users

282 Many programming languages are based on the programming paradigm of Object-Oriented
283 Programming (OOP), wherein individual components of the program resemble “reusable objects”
284 with defined input and output parameters (**Figure 3a**). This compartmentalization allows the
285 programmer to assemble these “objects” in any manner to accomplish the task at hand provided the
286 requisite parameters are met for individual objects. In the same spirit as OOP, ChIP-AP has been
287 designed to be “object-oriented” in nature (**Figure 3b**).

288

289 To instantiate a ChIP-AP run, all input arguments are passed through the command line or the
290 graphical interfaces. What is essential for a run is the location of the input sequencing files (raw fastq)
291 and a settings table for customization of pipeline constituent programs (discussed in the following
292 section) (**Figure 3b**). ChIP-AP then proceeds to then construct a folder hierarchy and places within
293 each folder the corresponding sub-script for that stage of analysis. Each ChIP-AP sub-script script is
294 in essence an instantiated object with defined input and output parameters passing files sequentially
295 from one folder to the next for processing and analysis. Should a user wish to add to or remove an
296 aspect of the pipeline, one simply needs to be mindful of the adjoining objects input/output
297 characteristics. ChIP-AP therefore provides an analysis platform wherein individual analysis steps can
298 be modularly swapped with equivalent steps, provided they have identical input and output

299 characteristics, without requiring additional changes to the flow of analysis or code. This
300 compartmentalization of analytical steps enables ChIP-AP to be exponentially customizable to
301 differing scenarios if the user is proficient enough to code the equivalent analysis step required. The
302 ChIP-AP documentation on GitHub accurately outlines all the analysis steps and documents the input
303 and output behaviours of each sub-script, this is in addition to a comprehensively commented master
304 script outlining the same information in code.

305

306 **Constituent Program Customization and Analysis Reproducibility Through the Settings Table**

307 The lack of result reproducibility in science is a major and on-going issue³⁵. The field has continued to
308 change and adapt to this problem with journals enforcing stricter reporting of materials and methods
309 in an attempt to curtail such issues. Unfortunately, bioinformatics methods reporting is an area of
310 scientific research where significant work is still required. Reporting of ChIP-Seq analyses in
311 publications consistently lacks necessary details with many authors omitting key program
312 modification parameters or even neglecting to mention key analysis steps entirely. We have therefore
313 attempted to address this issue by ensuring ChIP-AP analyses are reproducible through an accurate
314 and consistent means of reporting.

315

316 A key design aspect of ChIP-AP was to require the provision of a Settings Table (ST). If no table is
317 provided, ChIP-AP will use a pre-defined default-ST (DST; **Table 2**). The ST lists all the programs
318 used in the ChIP-AP run and all the necessary optional program arguments entered for that particular
319 run. It is therefore a listing of all non-hard-coded program modification parameters/flags used for a
320 particular analysis. For ChIP-AP to reproduce any analysis, it simply needs the raw sequencing fastq
321 files and the ST used. *We consider the dissemination of the information contained in the ST as both*
322 *vital and essential, along with results obtained.* The ST can be included as a supplemental table in a
323 manuscript or can be included as a processed data file when submitting data to an upload repository
324 like GEO. In either case, the information of this file *must* be presented when publishing data to ensure
325 analysis reproducibility in a format that is both consistent and convenient. Of note also, whether the

326 user provided a ST as input or the default-ST was used, a copy of the table will be found in the output
327 folder to ensure all required program modification parameters are provided accompanying the final
328 result.

329

330 ChIP-AP User Interfaces for Biologists

331 There is an ever-increasing need to make dry-lab analyses accessible to wet-lab biologists wishing to
332 investigate and interrogate data themselves without having to collaborate with (or wait for) a
333 bioinformatician. This is straightforward if a single program is required for an analysis like GraphPad
334 Prism or SAS. However, longer or more comprehensive analyses and workflows would typically
335 require a degree of coding to work. It is in this domain that ChIP-Seq analysis resides as it requires
336 the utilization of multiple programs, each feeding into each other to perform a coherent analysis. In an
337 attempt to address this demand, platforms such as Galaxy, or licensed software such as the Partek
338 Genomics Suite, have been developed to add graphical user interface (GUI) elements to analyses to
339 make higher-level analyses more accessible to researchers with no coding background. These
340 platforms though, particularly for ChIP-Seq analyses, utilize only a single peak caller and can offer
341 limited customization of program parameters in certain scenarios. As discussed, this can result in
342 incomplete analysis of the bound landscape owing to algorithmic limitations and biases, issues
343 ChIP-AP was designed to address. It was therefore necessary for ChIP-AP to incorporate its own GUI
344 to aide users in completing their required analyses and thus enable researchers with no coding
345 experience to perform independent analyses.

346

347 To address the breadth of computer proficiencies seen in the wet-lab scientific community, we
348 implemented two GUI's, the choice of which to use will depend on a user's proficiency with
349 ChIP-AP. Through the guided step-by-step tutorials found on our Github, users can install ChIP-AP
350 on any modern operating system, including Windows 10, and run the GUI of their choosing. The
351 GitHub repository lists the system hardware requirements to run ChIP-AP, but many modern laptops

352 and computers commonly purchased for research are capable of analysing data locally, without
353 needing dedicated server hardware.

354

355 For users unfamiliar with the command line, we have implemented the Wizard interface (**Figure 3c**),
356 inspired by installation wizards from the Windows 95/98 era of computing. The ChIP-AP wizard will
357 guide users through the analysis configuration by means of a series of panels each asking a single
358 question about the input data. On completion, users will have provided all the necessary information
359 required for a ChIP-AP run and can start their analysis directly from the wizard. This GUI
360 implementation was designed to not overwhelm users with multiple questions simultaneously asking
361 for input, but rather asks for data in a more guided approach.

362

363 For users familiar with the input requirements of ChIP-AP, we have implemented the Dashboard
364 interface (**Figure 3d**). The dashboard asks the same questions as the wizard but in a single panel,
365 enabling users to input the required data more quickly (**Figure 3d – Data Input**). Once all the required
366 information is input, as with the wizard, users can run ChIP-AP directly from the interface. In stark
367 difference to the wizard though, the dashboard interface contains a command line translation window
368 at the bottom of the interface (**Figure 3d – Command Line Translation**). As users enter data in the
369 GUI elements, the command line translation window will automatically update to accommodate the
370 additional/changed inputs. This enables researchers to gradually draw connections between translating
371 static GUI elements into command line arguments and flags to modulate and control program
372 behaviour. Such an implementation will aide some researchers more comfortably and confidently
373 transition from GUI to command line usage of ChIP-AP, and hopefully, beyond for their research.

374

375 Finally, independent of whether a user opts to use the wizard or dashboard interface, users will be
376 prompted to either use the DST or choose to upload their own ST. As discussed, the functionality and

377 reproducibility provided by the DST/ST is essential for ChIP-AP reproducibility, thus enabling a GUI
378 utilizing researcher to reproduce an analysis performed and customized by a bioinformatician.

379

380 Conclusion

381 ChIP-Seq is a well-established experimental protocol for profiling DNA-interacting proteins. In the
382 computational space, many software tools have been developed with over 50 peak callers being
383 published to date. Despite the abundance of available peak callers however, benchmarking studies
384 have consistently shown poor overlap between peak-sets from different peak callers. This is because
385 every caller has distinct selectivity and specificity characteristics which are often not additive and
386 seldom completely overlap with other peak callers in many scenarios. Additionally, it has been
387 extensively shown that the performance of a peak caller is subject to the read characteristics and read
388 distributions of the dataset in question. An individual peak caller can outperform other callers in
389 certain datasets but will perform poorly in alternate datasets. Therefore, with the heterogeneity
390 observed in experimental samples arising from profiling different DNA-binding proteins each profiled
391 with differing immunoprecipitation and library preparation protocols, reliance on a single peak caller
392 is unlikely to yield the most reliable, consistent or comprehensive results.

393

394 To circumvent the limitations and biases of individual peak callers, we rationalized that integrating
395 the results of multiple peak callers would yield improved peak calling consistency, confidence and
396 more comprehensively assess the binding landscape without requiring additional wet-lab
397 observations. As such, we developed the integrated ChIP-Seq analysis pipeline, ChIP-AP, which takes
398 design decisions from established workflows such as those utilized in consortia projects like
399 ENCODE¹⁸. ChIP-AP has been coded from the ground-up to be as simple to use as possible for users
400 inexperienced with the command line by providing two GUI's for use, the wizard or dashboard.
401 ChIP-AP still however remains exponentially customizable for advanced of users by facilitating
402 fine-grained customization of constituent programs through the ST, or, through its provision of
403 customizable modular framework that enables swapping of analysis stages to tailor ChIP-AP for

404 custom workflows. While ChIP-AP has been designed and written specifically for ChIP-Seq analysis,
405 the framework and design principles on which its coded, facilitate its adaptation and use for other
406 existing (ATAC-Seq^{36,37}, RIP-Seq³⁸, Cut&Run³⁴) and future emerging technologies. Should a new,
407 peak caller or analytical tool be developed, minimal changes are required to add an additional step in
408 the pipeline to accommodate the inclusion of said tool. This allows ChIP-AP to be easily modified to
409 work with emerging techniques and any tools that will be specifically developed for such a technique.
410 ChIP-AP can therefore be expanded or enhanced to suit future applications and uses with necessary
411 program arguments being passed through the settings table for each ChIP-AP run. To the best of our
412 research, we have yet to find an integrated software solution currently available that utilizes multiple
413 peak callers other than ChIP-AP.

414

415 ChIP-AP as presented here though, allows users to sub-set the binding landscape in a manner that is
416 best suited to address their biological research question, while allowing users to switch between
417 differing sub-sets depending on the question at hand. By utilizing the consensus peak set, binding
418 motif accuracy can be significantly increased by restricting the motif search space to only the most
419 confident peaks. This also has improved outcomes when attempting down-stream GO analysis
420 wherein more targeted and biologically significant terms can be reported. In contrast though, if the
421 profiled dataset has unfavourable characteristics such as poor enrichment or shows high signal:noise,
422 the union peak set can potentially yield improved results and allow users to marginally sacrifice
423 specificity for a potentially significant increase in sensitivity across the binding landscape. In between
424 these two extremes of data sub-sets is a gradient of sensitivity thresholds that can be selected
425 depending on the biological question and the presence of additional, supportive data from independent
426 techniques and methodologies. By reporting such an integrated analysis, ChIP-AP enables the end
427 user to focus on the biological question at hand by providing a comprehensive protein binding profile
428 without needing data re-analysis. ChIP-AP can therefore provide both substantial improvements to
429 peak capturing and analysis reliability from a single integrated and comprehensive analysis.

430

431 **Materials and Methods**

432 **ChIP-AP Constituent Programs**

433 ChIP-AP is an integrated pipeline that brings multiple command line programs together into a single,
434 seamless and easy to use pipeline. At time of publication, these include FastQC³⁹, Clumpify and
435 BBDuk from the BBMap Suite⁴⁰, Trimmomatic⁴¹, BWA⁴², Samtools⁴³, deepTools⁴⁴, MACS2⁴⁵,
436 GEM¹⁶, SICER2⁴⁶, HOMER¹⁵ and Genrich¹³. If using ChIP-AP, please cite all constituent tools as
437 well. It is best to refer to the GitHub repository for the latest citation list which would include any
438 additional tools incorporated into ChIP-AP since publication.

439

440 **SNU-398 Culturing**

441 SNU-398 cell line was obtained from the American Type Culture Collection (ATCC). The cells were
442 maintained in RPMI medium supplemented with 10% foetal bovine serum (FBS) at 37°C in a
443 humidified atmosphere of 5% CO₂ as recommended by ATCC.

444

445 **SALL4 ChIP-Seq Preparation and Sequencing**

446 20 million SNU-398 cells were cross-linked with 1% formaldehyde for 10 minutes at room
447 temperature. The reaction was terminated by adding 2M glycine to a final concentration of 125mM.
448 Cells were then washed with 1×PBS and resuspended in 1mL of cell lysis buffer (20mM Tris pH8.0,
449 85mM KCl, 0.5% nonidet P-40, protease inhibitor). After 10 minutes of incubation on ice, cells were
450 spun down and cell pellet was resuspended in another 1mL of cell lysis buffer. After another 5
451 minutes of incubation on ice, cells were spun down and cell pellet was resuspended in 1mL of nuclear
452 lysis buffer (10mM Tris-HCl pH7.5, 1% nonidet P-40, 0.5% sodium deoxycholate, 0.1% SDS,
453 protease inhibitor). After 10 minutes of incubation on ice, chromatin was sheared to 500bp.
454 Antibody-protein A/G Dynabead conjugate was prepared by adding 0.75µg of SALL4 rabbit
455 monoclonal antibody (Cell Signaling Technology #8459) to pre-washed 50µL of protein A/G
456 Dynabeads (Life Techonologies) with one hour incubation at 4°C with rotation. Sheared chromatin was
457 then added to antibody-protein A/G conjugate and incubated overnight at 4°C with rotation. After
458 overnight incubation, the beads were washed sequentially with the following buffers: twice with

459 RIPA/500mM NaCl buffer (0.1% deoxycholate, 0.1% SDS, 1% Triton X-100, 500mM NaCl, 1mM
460 EDTA, 20mM Tris-HCl pH8.1), twice with LiCl buffer (0.25M LiCl, 1% nonidet P-40, 1% sodium
461 deoxycholate, 1mM EDTA, 10mM Tris-HCl pH8.1), twice with TE buffer (10mM Tris-HCl pH8.0,
462 1mM EDTA pH8.0). Protein complexes were reverse cross-linked with 50 μ L of ChIP Elution Buffer
463 (10mM Tris-HCl pH8.0, 5mM EDTA, 300mM NaCl, 0.1% SDS) and 8 μ L of Reverse Crosslink Mix
464 (250mM Tris-HCl pH6.5, 1.25M NaCl, 62.5mM EDTA, 5mg/mL proteinase K, 62.5 μ g/mL RNase A)
465 at 65°C for 5 hours. Reverse cross-linked DNA was cleaned up using SPRI beads (Beckman Coulter)
466 and eluted in 10mM Tris-HCl pH 8.0. To generate libraries for deep sequencing, the eluted DNA was
467 end-repaired using End-It DNA End-Repair Kit (Epicenter #ER0720) and A-tailing was then carried
468 using Klenow (3'-5' exo-) enzyme (New England Biolabs). Illumina sequencing adaptors were ligated
469 to the DNA fragments and adaptor-ligated DNA fragments were enriched with 14 cycles of PCR.
470 DNA libraries were gel purified and analyzed on Bioanalyzer (Agilent) for their size distribution.
471 Libraries were sequenced on Illumina HiSeq 2500 sequencer with single-end 35bp settings. The
472 sequencing and processed files have been uploaded to GEO with Accession number xxxx (reviewer
473 access token xxxx).

474

475 SALL4 ChIP-Seq Analysis and Comparisons

476 The generated SALL4 ChIP-Seq was processed with ChIP-AP (v4.1) using a hg38 genome. The
477 settings table used for analysis is found below.

Program	Argument
fastqc1	-q
clumpify	dedupe spany addcount
bbduk	ktrim=1 hdist=2
trimmomatic	LEADING:20 SLIDINGWINDOW:4:20 TRAILING:20 MINLEN:20
fastqc2	-q
bwa_mem	
samtools_view	
plotfingerprint	-bs 50 --centerReads --ignoreDuplicates
fastqcs3	-q
macs2_callpeak	
gem	-Xmx30G --k_min 8 --k_max 12
sicer2	
homer_findPeaks	
genrich	--adjustp -v

homer_mergePeaks	
homer_annotatePeaks	
fold_change_calculator	--normfactor uniquely_mapped

478

479 For all analyses, the union peak set was utilized. The fingerprint plot (Figure 2a) was generated as part
480 of the ChIP-AP run with the flags outlined in the settings table. The upset plot (Figure 2b) was
481 generated by taking the “venn.txt” data from the ChIP-AP run output (folder 21_peaks_merging) and
482 plotting it in R⁴⁷ (v4.0.3) with the UpSetR⁴⁸ (v1.4.0) package.

483 For comparisons with the Cut&Run data, the Cut&Run data was processed as outlined previously³³
484 and is available from GEO, Accession GSE136332. To overlap the Cut&Run replicates, HOMER’s
485 mergePeaks was used with flags “-d 1500.” Next, the Cut&Run peaks identified in at least 2 replicates
486 were combined into a single list and compared to the SALL4 ChIP-Seq union peak set using
487 HOMER’s mergePeaks with flag “-d 2000”, this provided the list of overlapping regions, the number
488 of which was plotted in R⁴⁷ (v4.0.3) with the VennDiagram⁴⁹ (v1.6.20) package.

489 For the directed motif search within the SALL4 ChIP-Seq union peak set, HOMER’s¹⁵
490 findMotifsGenome function was used with flags “-find sall4_weighted_motif.motif.” For the
491 HOMER *de novo* motif search, HOMER’s findMotifsGenome function was used with flags “hg38 -
492 size given -mask.” For the MEME-ChIP (and sub-program²²⁻²⁴) motif search, first the union peak list
493 was processed with HOMER’s findMotifsGenome function with flag “-dumpFasta” to extract the
494 central 200bp sequences of each peak. HOMER also generated an equivalent set of background
495 sequences with comparable GC content to be used. Next, MEME-ChIP was run with flags “-neg
496 background.fa -meme-nmotifs 25 union_peaks.fa.” Motif logo files were generated using R⁴⁷ (v4.0.3)
497 and the seqLogo⁵⁰ (v1.52.0) package.

498 The gene ontology analysis of the SALL4 ChIP-Seq dataset performed was part of the ChIP-AP run
499 using the flag “-goann” which utilizes HOMER to perform the analysis following peak annotation. To
500 compare with the processed SALL4 knock-down results published³³, we started from supplemental
501 tables 4 and 5 from the publication. Next, we overlaid the reported gene names from the SALL4
502 ChIP-Seq union peak set to those gene lists to determine overlapping gene names.

503

504 **Encode Datasets Utilized and Processing**

505 A number of ENCODE datasets were downloaded and utilized for our analysis. The table below lists

506 all the downloaded experiment ID's used. Data was downloaded from ENCODE March 2021.

Cell Line	Transcription Factor	ChIP Experiment ID's	Control Experiment ID's
GM12878	MAX	ENCFF000VXY ENCFF000VYA	ENCFF000VWF ENCFF000VWH
	SPI1	ENCFF000VXY ENCFF000VYA	
HepG2	ZBTB33	ENCFF000PSP ENCFF000PSW	ENCFF000POC ENCFF000POH
	CEBPB	ENCFF000XQM ENCFF000XQN	
K562	MAFF	ENCFF000YSQ ENCFF000YSS	ENCFF002EFF ENCFF002EFD
	JUN	ENCFF000YJJ ENCFF000YJL	
	GATA1	ENCFF000YND ENCFF000YNF	
	MEIS2	R1: ENCFF002EIU ENCFF002EIW R2: ENCFF002EIV ENCFF002EIX	R1: ENCFF002EFF ENCFF002EFD R2: ENCFF002EFH ENCFF002EFA
	RUNX1	R1: ENCFF002DOZ ENCFF002EGD R2: ENCFF002EGE ENCFF002DPH	
	ATF4	R1: ENCFF081USS ENCFF565KLI R2: ENCFF069VNL ENCFF682IGK	

507

508 All ENCODE datasets were processed with ChIP-AP (v4.1) with the following settings table

Program	Argument
fastqc1	-q
clumpify	dedupe spany addcount qout=33 fixjunk
bbduk	ktrim=1 hdist=2
trimmomatic	LEADING:20 SLIDINGWINDOW:4:20 TRAILING:20 MINLEN:20
fastqc2	-q
bwa_mem	
samtools_view	
plotfingerprint	-bs 50 --centerReads --ignoreDuplicates
fastqcs3	-q
macs2_callpeak	
gem	-Xmx30G --k_min 8 --k_max 12
sicer2	
homer_findPeaks	
genrich	--adjustp -v

homer_mergePeaks	
homer_annotatePeaks	
fold_change_calculator	--normfactor uniquely_mapped

509 For each transcription factor, the corresponding JASPAR binding motif for the cell line in question
510 was downloaded from MethMotif¹⁹ and manually converted to HOMER motif format. For the
511 directed motif searches, HOMER's findMotifsGenome was utilized with flags "hg38 -find
512 binding_motif.motif." For HOMER *de novo* motif discovery, the findMotifsGenome program was
513 used with flags "hg38 -size given -mask -dumpFasta." This ran the motif discovery while also giving
514 the necessary fasta sequence files (target.fa and background.fa) required to run the MEME-Suite. The
515 MEME *de novo* motif discovery was run with flags "-neg background.fa -meme-nmotifs 25 target.fa."
516 Motif logo files were generated using R⁴⁷ (v4.0.3) and the seqLogo⁵⁰ (v1.52.0) package. The gene
517 ontology results were generated as part of HOMER's annotatePeaks function for the required peak
518 sets. HOMER annotatePeaks was utilized with a known motif provided with -m flag to include the
519 distances from all starting coordinate motif instances in each peak to their respective peak starting
520 coordinate. A custom script was utilized to extract the distances from every peak's weighted peak
521 center coordinate to the midpoint coordinate of the motif instance closest to the weighted peak center.
522 The density plots representing this data were generated using R⁴⁷ and the ggplot2⁵¹. Peak-Motif
523 percentages were plotted using Graphpad Prism v9.1.0.
524

525 Figure and Table Legends

526 Figure 1 – Consensus peak set improves detected motif accuracy

527 a) Peak-Motif percentage (number of peaks with binding motif) for all 10 TF's profiled as identified
528 for the MACS2 and the consensus peak sets. b) The motif position-bias for CEBPB, JUN, SPI1 and
529 ZBTB33 for the consensus peak set and the individual peak callers. The position-bias is a measure of
530 how far the identified motif sits away from the weighted peak center. c) The CEBPB *de novo* motif
531 discovery results as reported by HOMER for the consensus peak set. The line above the peaks
532 delineates position of the binding motif. d) The CEBPB *de novo* motif discovery results as reported by
533 HOMER for the MACS2 peak set. The line above the peaks delineates position of the binding motif.
534 e) The MAFF *de novo* motif discovery results as reported by HOMER for the consensus peak set. The
535 line above the peaks delineates position of the binding motif. f) The MAFF *de novo* motif discovery
536 results as reported by HOMER for the MACS2 peak set. The line above the peaks delineates the
537 position of the binding motif.

538

539 Figure 2 – Union peak set comprehensiveness and accuracy

540 a) Fingerprint plot for aligned sequence files for samples. Negligible separation between the SALL4
541 and control curves indicates poor enrichment in the SALL4 samples. b) Upset plot describing the
542 distribution of peaks observed by each peak caller. The left histogram represents the total number of
543 called peaks per caller. The top histograms represent the size of the sub-sets in question. The
544 connected circles represent highlighted overlap. c) Venn diagram showing the overlapping number of
545 peaks between the SALL4 union ChIP-Seq dataset and the Cut&Run dataset. d) The motif sequence
546 used for the directed motif search in the SALL4 ChIP-Seq union set, which was found in 55.2% of the
547 union set. e) The STREME *de novo* motif search for the SALL4 union peak set identified the AT-rich
548 binding motif as the 2nd result. f) The HOMER *de novo* motif search for the SALL4 union peak set
549 identified the AT-rich binding motif as the 3rd result. g) The STREME identified motif (shown in d)
550 was found centrally enriched in the union peak set as compared to background sequences.

551

552 Figure 3 – Object Oriented Nature of ChIP-AP

553 a) In OOP, an abstract “object” is defined as a segment of code that accepts defined inputs, processes
554 the data, and outputs the data in a defined manner. Objects can then be combined in any manner to
555 produce desired output. b) ChIP-AP was designed to be “object-oriented” in nature with each stage of
556 analysis in a folder (01, 02...) having defined input/output characteristics. c) The ChIP-AP wizard
557 interface guides users through a series of windows, each asking for a single piece of input, till all
558 required information is gathered for a ChIP-AP run. d) The dashboard interface can be separated into
559 2 regions, the data input and command line translations segments. In the data input section, all the

560 required data for a ChIP-AP run is input from a single interface. The command line translation
561 window at the bottom dynamically changes as input is entered in the data input section, translating
562 static GUI elements into the necessary command line arguments/flags enabling users to view how
563 ChIP-AP's input is modified based on the provided input.

564

565 [Supplemental Figure 1](#)

566 a) The motif position-bias for ATF4, GATA1, MAFF, MAX, MEIS2 and RUNX1 for the consensus
567 peak set and the individual peak callers. The position-bias is a measure of how far the identified motif
568 sits away from the weighted peak center. b) The CEBPB *de novo* motif discovery results as reported
569 by the MEME-Suite for the consensus peak set. Above each p-value is which sub-program of MEME
570 called the said motif. c) The CEBPB *de novo* motif discovery results as reported by the MEME-Suite
571 for the MACS2 peak set. Above each p-value is which sub-program of MEME called said motif. d)
572 The MAFF *de novo* motif discovery results as reported by the MEME-Suite for the consensus peak
573 set. Above each p-value is which sub-program of MEME called said motif. The 6th result shows a
574 characteristic heterodimer binding profile for MAFF. e) The MAFF *de novo* motif discovery results as
575 reported by the MEME-Suite for the MACS2 peak set. Above each p-value is which sub-program of
576 MEME called said motif.

577

578 [Supplemental Figure 2](#)

579 a) Venn diagrams highlighting the degree of overlap between each individual callers peak-set and the
580 Cut&Run peak set, and the relatively few peaks called by each individual peak caller. b) The
581 MEME-ChIP results highlighting showing the correct AT-rich binding motif for SALL4 is the 3rd
582 called motif hit. The 2nd motif hit also is an AT-rich motif with near identical sequence.

583

584 [Table 1 – Top 20 RUNX1 GO Terms](#)

585 The top 20 RUNX1 GO terms returned for the consensus peak set (left) and the MACS2 peak set
586 (right). The consensus peak set GO returned GO terms are more directly relatable to defined RUNX1
587 functions as compared to the MACS2 results.

588

589 [Table 2 – Default Settings Table for ChIP-AP](#)

590 The default program settings table used by ChIP-AP if no user provided settings table is provided.
591 The left column lists the constituent programs of ChIP-AP with their optional modification
592 parameters/flags found in the right column.

593

594 **Supplemental Table 1**

595 Table listing and overview of all the profiled TF's, their TF family and cell line of origin. The table
596 also lists the total number of peaks found in the MACS2 and consensus peak sets, along with the
597 peak-motif percentages for each set.

598

599 **Supplemental Table 2**

600 A listing of the z-tests performed testing the position-bias distributions of the consensus peak set
601 compared to each individual peak caller. Significant differences are highlighted in green. Cells
602 highlighted yellow indicate values approaching significance.

603

604 **Supplemental Table 3**

605 All the consensus peak GO results for all 10 TF's (1 sheet per TF).

606

607 **Supplemental Table 4**

608 All the MACS2 peak GO results for all 10 TF's (1 sheet per TF).

609

610 **Supplemental Table 5**

611 The union peak-list for the SALL4 ChIP-seq

612

613 **Supplemental Table 6**

614 The peak-motif percentages for each individual peak callers results in the SALL4 ChIP-Seq dataset.

615

616 **Supplemental Table 7**

617 The GO results for the SALL4 union peak-set.

618

619 **Supplemental Table 8**

620 The differentially expressed genes from the SALL4 knock-down RNA-Seq experiment found to
621 contain at least 1 peak in the SALL4 union peak-set.

622

623 Acknowledgements

624 The authors would like to thank Yanjing V. Liu, Giorgia Maroni, Elena Levantini, Chenxi Qiu and
625 Bon Q. Trinh for their feedback on the CHIP-AP installation guides and installations. We want to
626 thank them for letting us use their laptops and computers as test-beds to ensure our software is as
627 seamless as possible for others to use. We also want to thank Robert Welner for his feedback on the
628 manuscript. We want to especially thank Touati Benoukraf for his insightful discussions and
629 comments regarding CHIP-AP, its development and its presentation.

630

631 Contributions

632 J.S. and M.A.B designed the package. J.S. was the lead programmer. J.S. and M.A.B tested,
633 optimized and debugged CHIP-AP. D.E.T and KJ.Y. performed the SALL4 CHIP-Seq. J.S., D.G.T and
634 M.A.B interpreted results and wrote the manuscript. M.A.B conceived and directed the project.

635 References

- 636 1 Collas, P. The current state of chromatin immunoprecipitation. *Mol Biotechnol* **45**, 87-100,
637 doi:10.1007/s12033-009-9239-8 (2010).
- 638 2 Johnson, D. S., Mortazavi, A., Myers, R. M. & Wold, B. Genome-wide mapping of in vivo
639 protein-DNA interactions. *Science* **316**, 1497-1502, doi:10.1126/science.1141319 (2007).
- 640 3 Bernstein, B. E. *et al.* Genomic maps and comparative analysis of histone modifications in
641 human and mouse. *Cell* **120**, 169-181, doi:10.1016/j.cell.2005.01.001 (2005).
- 642 4 Park, P. J. ChIP-seq: advantages and challenges of a maturing technology. *Nat Rev Genet* **10**,
643 669-680, doi:10.1038/nrg2641 (2009).
- 644 5 Barski, A. *et al.* High-resolution profiling of histone methylations in the human genome. *Cell*
645 **129**, 823-837, doi:10.1016/j.cell.2007.05.009 (2007).
- 646 6 Mikkelsen, T. S. *et al.* Genome-wide maps of chromatin state in pluripotent and lineage-
647 committed cells. *Nature* **448**, 553-560, doi:10.1038/nature06008 (2007).
- 648 7 Chen, Y. *et al.* Systematic evaluation of factors influencing ChIP-seq fidelity. *Nat Methods* **9**,
649 609-614, doi:10.1038/nmeth.1985 (2012).
- 650 8 Kurzawa, N., Eils, R., Steinhauser, S. & Herrmann, C. A comprehensive comparison of tools
651 for differential ChIP-seq analysis. *Briefings in Bioinformatics* **17**, 953-966,
652 doi:10.1093/bib/bbv110 (2016).
- 653 9 Laajala, T. D. *et al.* A practical comparison of methods for detecting transcription factor
654 binding sites in ChIP-seq experiments. *BMC Genomics* **10**, 618, doi:10.1186/1471-2164-10-
655 618 (2009).
- 656 10 Wilbanks, E. G. & Facciotti, M. T. Evaluation of algorithm performance in ChIP-seq peak
657 detection. *PLoS One* **5**, e11471, doi:10.1371/journal.pone.0011471 (2010).
- 658 11 Koohy, H., Down, T. A., Spivakov, M. & Hubbard, T. A comparison of peak callers used for
659 DNase-Seq data. *PLoS One* **9**, e96303, doi:10.1371/journal.pone.0096303 (2014).
- 660 12 Jeon, H., Lee, H., Kang, B., Jang, I. & Roh, T. Y. Comparative analysis of commonly used
661 peak calling programs for ChIP-Seq analysis. *Genomics Inform* **18**, e42,
662 doi:10.5808/GI.2020.18.4.e42 (2020).
- 663 13 Gaspar, J. *Genrich: detecting sites of genomic enrichment*,
664 <<https://github.com/jsh58/Genrich>> (
665 14 Liu, T. Use model-based Analysis of ChIP-Seq (MACS) to analyze short reads generated by
666 sequencing protein-DNA interactions in embryonic stem cells. *Methods Mol Biol* **1150**, 81-
667 95, doi:10.1007/978-1-4939-0512-6_4 (2014).
- 668 15 Heinz, S. *et al.* Simple combinations of lineage-determining transcription factors prime cis-
669 regulatory elements required for macrophage and B cell identities. *Mol Cell* **38**, 576-589,
670 doi:10.1016/j.molcel.2010.05.004 (2010).
- 671 16 Guo, Y., Mahony, S. & Gifford, D. K. High resolution genome wide binding event finding
672 and motif discovery reveals transcription factor spatial binding constraints. *PLoS Comput Biol*
673 **8**, e1002638, doi:10.1371/journal.pcbi.1002638 (2012).
- 674 17 Xu, S., Grullon, S., Ge, K. & Peng, W. Spatial clustering for identification of ChIP-enriched
675 regions (SICER) to map regions of histone methylation patterns in embryonic stem cells.
676 *Methods Mol Biol* **1150**, 97-111, doi:10.1007/978-1-4939-0512-6_5 (2014).
- 677 18 Consortium, E. P. An integrated encyclopedia of DNA elements in the human genome.
678 *Nature* **489**, 57-74, doi:10.1038/nature11247 (2012).
- 679 19 Xuan Lin, Q. X. *et al.* MethMotif: an integrative cell specific database of transcription factor
680 binding motifs coupled with DNA methylation profiles. *Nucleic Acids Res* **47**, D145-D154,
681 doi:10.1093/nar/gky1005 (2019).
- 682 20 Khan, A. *et al.* JASPAR 2018: update of the open-access database of transcription factor
683 binding profiles and its web framework. *Nucleic Acids Res* **46**, D260-D266,
684 doi:10.1093/nar/gkx1126 (2018).
- 685 21 Lin, Q. X. X., Thieffry, D., Jha, S. & Benoukraf, T. TFregulomeR reveals transcription
686 factors' context-specific features and functions. *Nucleic Acids Res* **48**, e10,
687 doi:10.1093/nar/gkz1088 (2020).

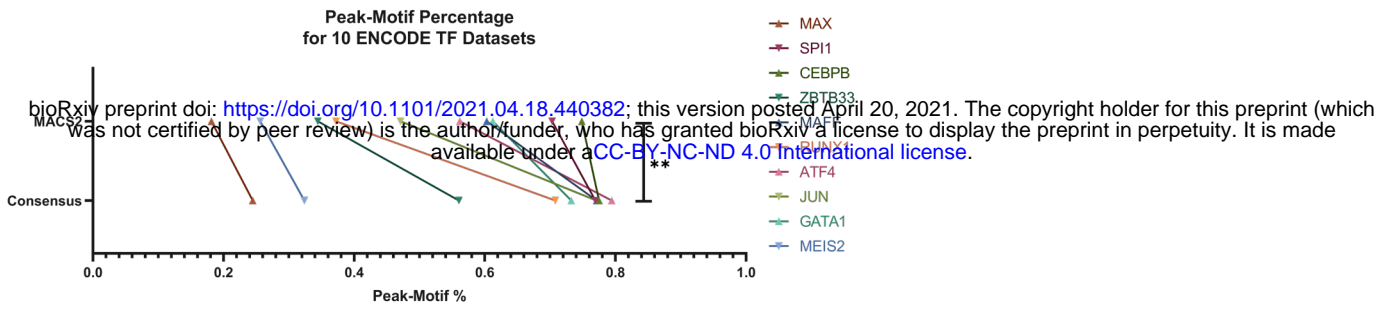
- 688 22 Bailey, T. L. STREME: Accurate and versatile sequence motif discovery. *bioRxiv*,
689 2020.2011.2023.394619, doi:10.1101/2020.11.23.394619 (2020).
- 690 23 Bailey, T. L. & Machanick, P. Inferring direct DNA binding from CHIP-seq. *Nucleic Acids*
691 *Res* **40**, e128, doi:10.1093/nar/gks433 (2012).
- 692 24 Machanick, P. & Bailey, T. L. MEME-CHIP: motif analysis of large DNA datasets.
693 *Bioinformatics* **27**, 1696-1697, doi:10.1093/bioinformatics/btr189 (2011).
- 694 25 Fuka, G. *et al.* Silencing of ETV6/RUNX1 abrogates PI3K/AKT/mTOR signaling and
695 impairs reconstitution of leukemia in xenografts. *Leukemia* **26**, 927-933,
696 doi:10.1038/leu.2011.322 (2012).
- 697 26 Imperato, M. R., Cauchy, P., Obier, N. & Bonifer, C. J. I. J. o. H. The RUNX1-PU.1 axis in
698 the control of hematopoiesis. **101**, 319-329, doi:10.1007/s12185-015-1762-8 (2015).
- 699 27 Lam, K. & Zhang, D. E. RUNX1 and RUNX1-ETO: roles in hematopoiesis and
700 leukemogenesis. *Front Biosci (Landmark Ed)* **17**, 1120-1139 (2012).
- 701 28 Pencovich, N., Jaschek, R., Tanay, A. & Groner, Y. Dynamic combinatorial interactions of
702 RUNX1 and cooperating partners regulates megakaryocytic differentiation in cell line
703 models. *Blood* **117**, e1-14, doi:10.1182/blood-2010-07-295113 (2011).
- 704 29 Polak, R. *et al.* Autophagy inhibition as a potential future targeted therapy for ETV6-
705 RUNX1-driven B-cell precursor acute lymphoblastic leukemia. *Haematologica* **104**, 738-748,
706 doi:10.3324/haematol.2018.193631 (2019).
- 707 30 Wang, X. *et al.* Runx1 prevents wasting, myofibrillar disorganization, and autophagy of
708 skeletal muscle. *Genes Dev* **19**, 1715-1722, doi:10.1101/gad.1318305 (2005).
- 709 31 Tatetsu, H. *et al.* SALL4, the missing link between stem cells, development and cancer. *Gene*
710 **584**, 111-119, doi:10.1016/j.gene.2016.02.019 (2016).
- 711 32 Zhang, X., Yuan, X., Zhu, W., Qian, H. & Xu, W. SALL4: an emerging cancer biomarker and
712 target. *Cancer Lett* **357**, 55-62, doi:10.1016/j.canlet.2014.11.037 (2015).
- 713 33 Kong, N. R. *et al.* Zinc Finger Protein SALL4 Functions through an AT-Rich Motif to
714 Regulate Gene Expression. *Cell Rep* **34**, 108574, doi:10.1016/j.celrep.2020.108574 (2021).
- 715 34 Skene, P. J. & Henikoff, S. An efficient targeted nuclease strategy for high-resolution
716 mapping of DNA binding sites. *Elife* **6**, doi:10.7554/eLife.21856 (2017).
- 717 35 Baker, M. *1,500 scientists lift the lid on reproducibility*, <[https://www.nature.com/news/1-
718 500-scientists-lift-the-lid-on-reproducibility-1.19970](https://www.nature.com/news/1-500-scientists-lift-the-lid-on-reproducibility-1.19970)> (2016).
- 719 36 Buenrostro, J. D., Giresi, P. G., Zaba, L. C., Chang, H. Y. & Greenleaf, W. J. Transposition of
720 native chromatin for fast and sensitive epigenomic profiling of open chromatin, DNA-binding
721 proteins and nucleosome position. *Nat Methods* **10**, 1213-1218, doi:10.1038/nmeth.2688
722 (2013).
- 723 37 Buenrostro, J. D., Wu, B., Chang, H. Y. & Greenleaf, W. J. ATAC-seq: A Method for
724 Assaying Chromatin Accessibility Genome-Wide. *Curr Protoc Mol Biol* **109**, 21 29 21-21 29
725 29, doi:10.1002/0471142727.mb2129s109 (2015).
- 726 38 Clark, S. J. *et al.* Genome-wide base-resolution mapping of DNA methylation in single cells
727 using single-cell bisulfite sequencing (scBS-seq). *Nat Protoc* **12**, 534-547,
728 doi:10.1038/nprot.2016.187 (2017).
- 729 39 (2015).
- 730 40 BMAP: A Fast, Accurate, Splice-Aware Aligner (USA, 2014).
- 731 41 Bolger, A. M., Lohse, M. & Usadel, B. Trimmomatic: a flexible trimmer for Illumina
732 sequence data. *Bioinformatics* **30**, 2114-2120, doi:10.1093/bioinformatics/btu170 (2014).
- 733 42 Li, H. & Durbin, R. Fast and accurate short read alignment with Burrows-Wheeler transform.
734 *Bioinformatics* **25**, 1754-1760, doi:10.1093/bioinformatics/btp324 (2009).
- 735 43 Li, H. *et al.* The Sequence Alignment/Map format and SAMtools. *Bioinformatics* **25**, 2078-
736 2079, doi:10.1093/bioinformatics/btp352 (2009).
- 737 44 Ramirez, F. *et al.* deepTools2: a next generation web server for deep-sequencing data
738 analysis. *Nucleic Acids Res* **44**, W160-165, doi:10.1093/nar/gkw257 (2016).
- 739 45 Zhang, Y. *et al.* Model-based analysis of CHIP-Seq (MACS). *Genome Biol* **9**, R137,
740 doi:10.1186/gb-2008-9-9-r137 (2008).

741 46 Zang, C. *et al.* A clustering approach for identification of enriched domains from histone
742 modification ChIP-Seq data. *Bioinformatics* **25**, 1952-1958,
743 doi:10.1093/bioinformatics/btp340 (2009).
744 47 R: A Language and Environment for Statistical Computing (R Foundation for Statistical
745 Computing, Vienna, Austria, 2021).
746 48 UpSetR: A More Scalable Alternative to Venn and Euler Diagrams for Visualizing
747 Intersecting Sets (2019).
748 49 VennDiagram: Generate High-Resolution Venn and Euler Plots (2018).
749 50 seqLogo: Sequence logos for DNA sequence alignments (2019).
750 51 ggplot2: Elegant Graphics for Data Analysis (2016).

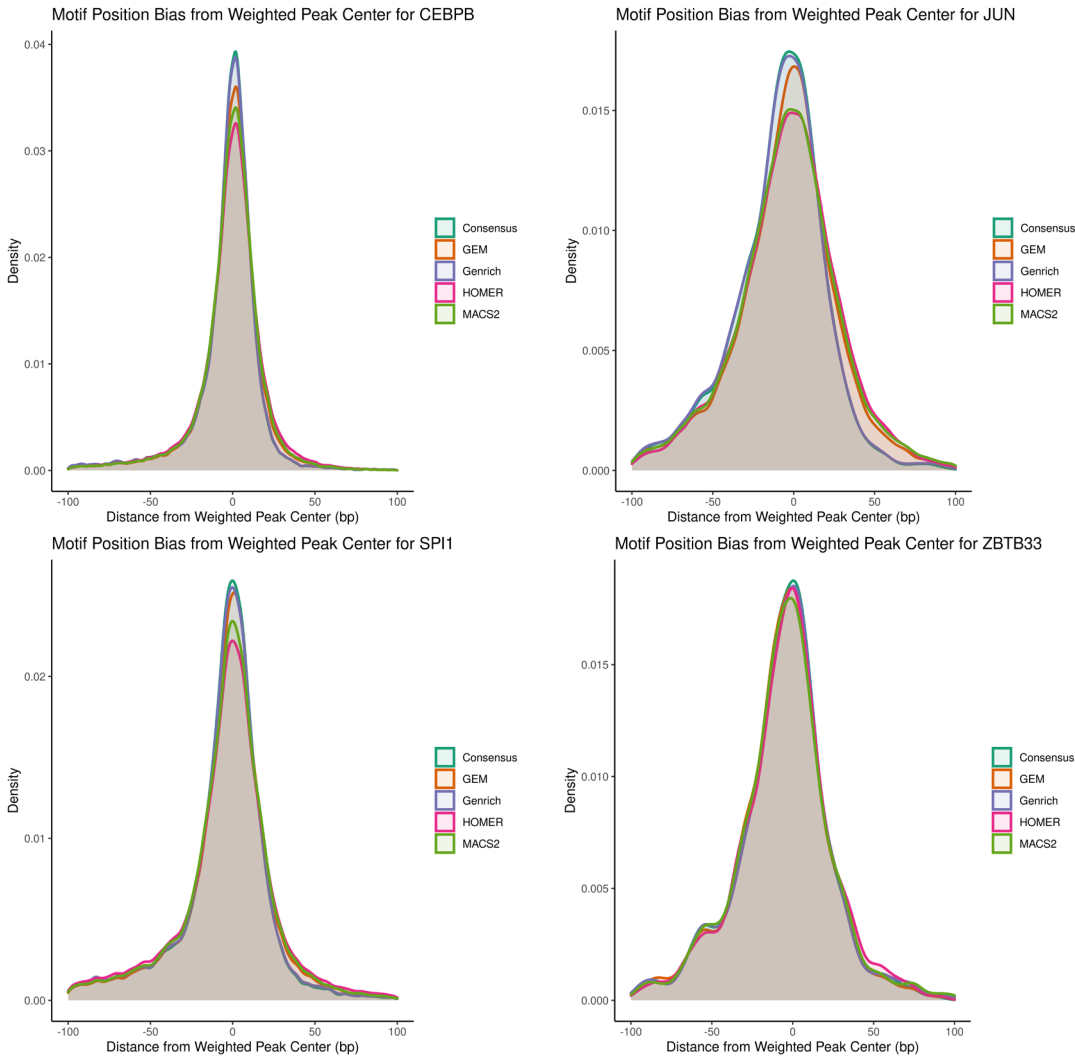
751

Figure 1

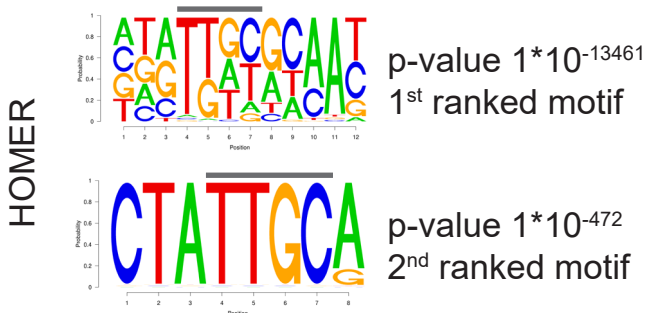
a



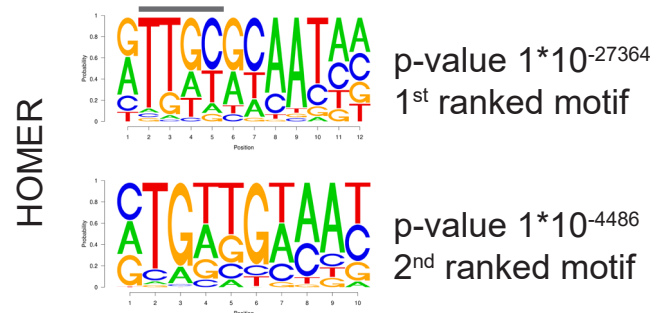
b



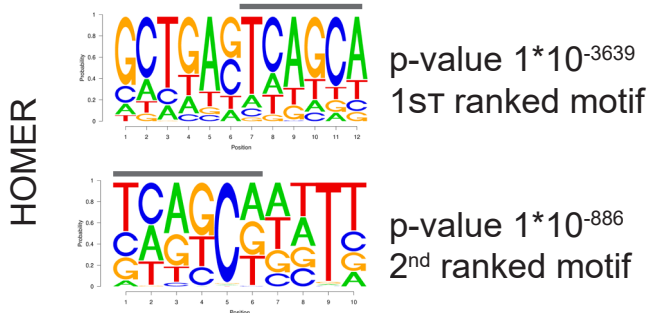
c CEBPB *De Novo* Motif Search - Consensus



d CEBPB *De Novo* Motif Search - MACS2



e MAFF *De Novo* Motif Search - Consensus



f MAFF *De Novo* Motif Search - MACS2

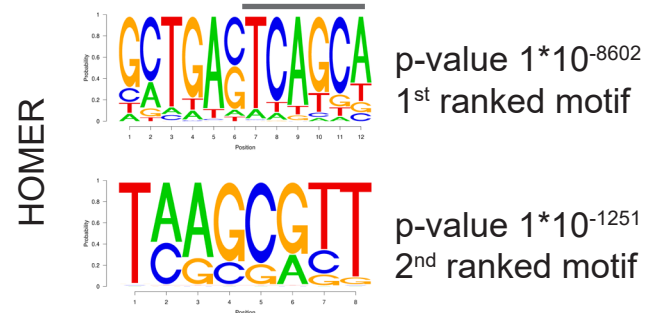
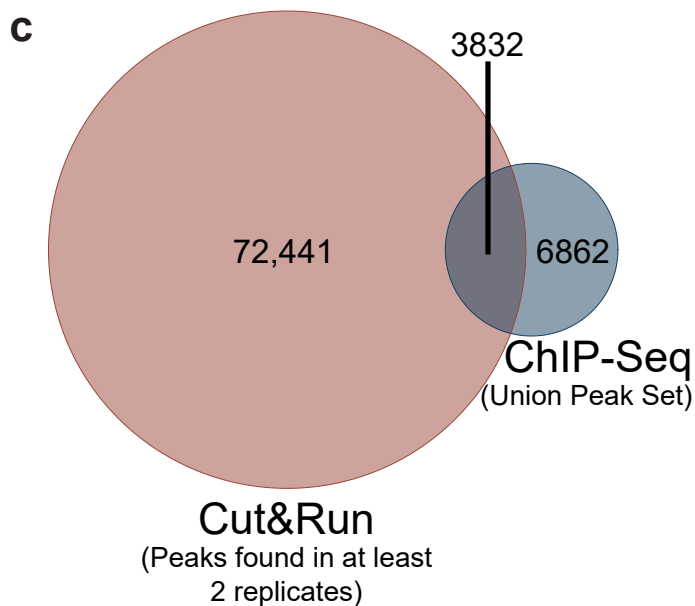
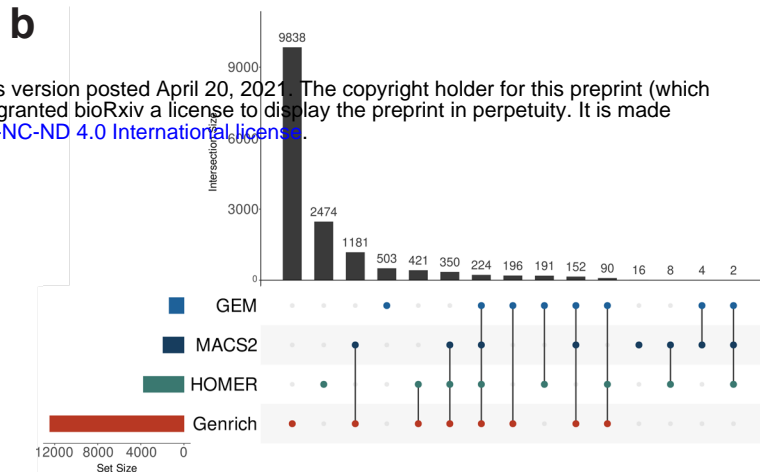
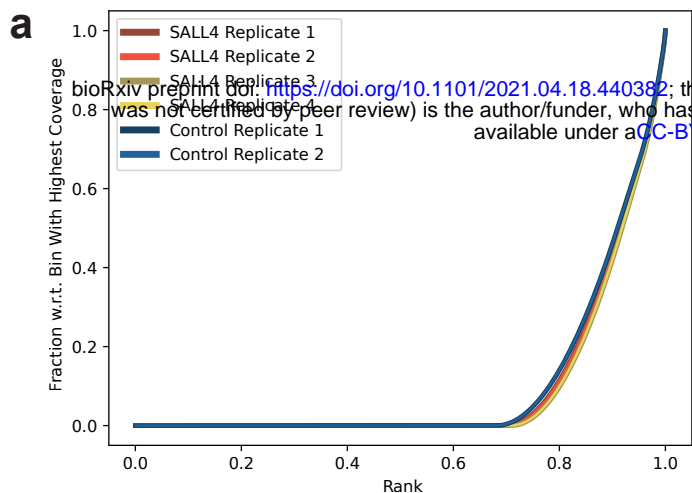
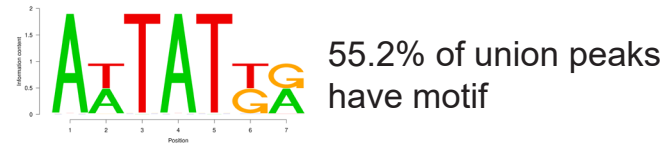


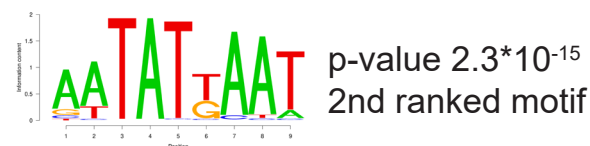
Figure 2



d Directed SALL4 Motif Search



e De Novo Motif Search - STREME



f De Novo Motif Search - HOMER

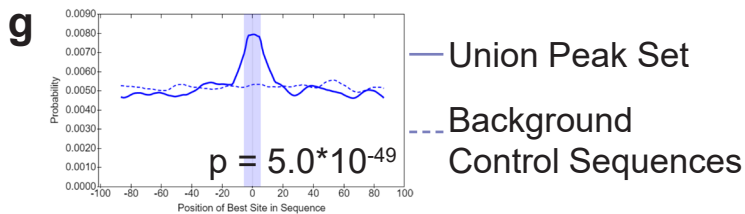
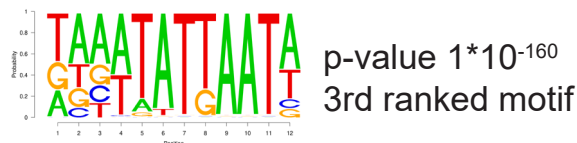
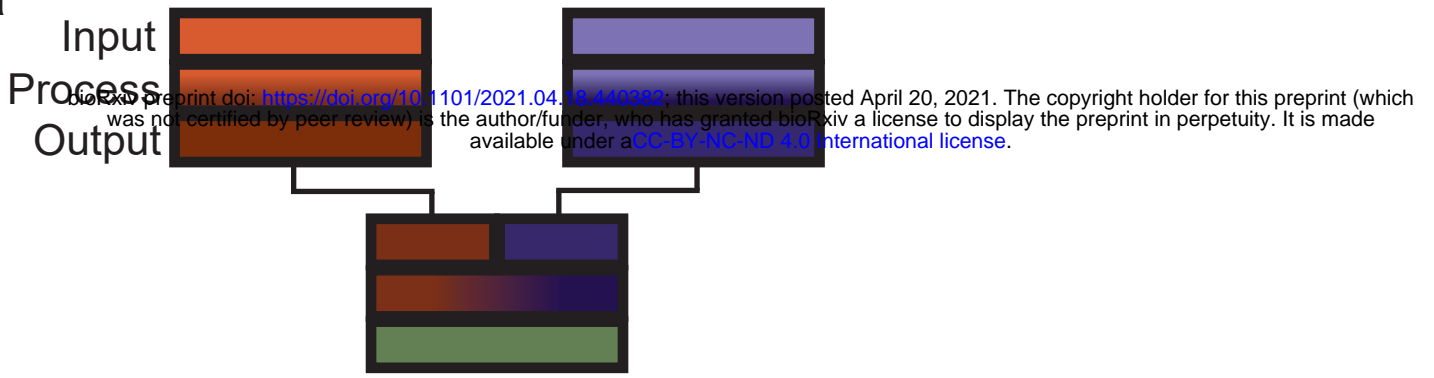
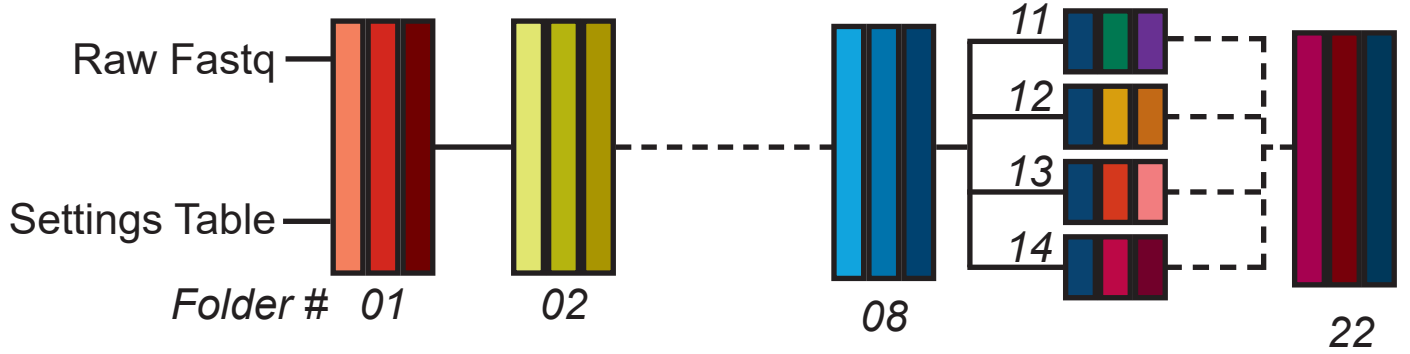


Figure 3

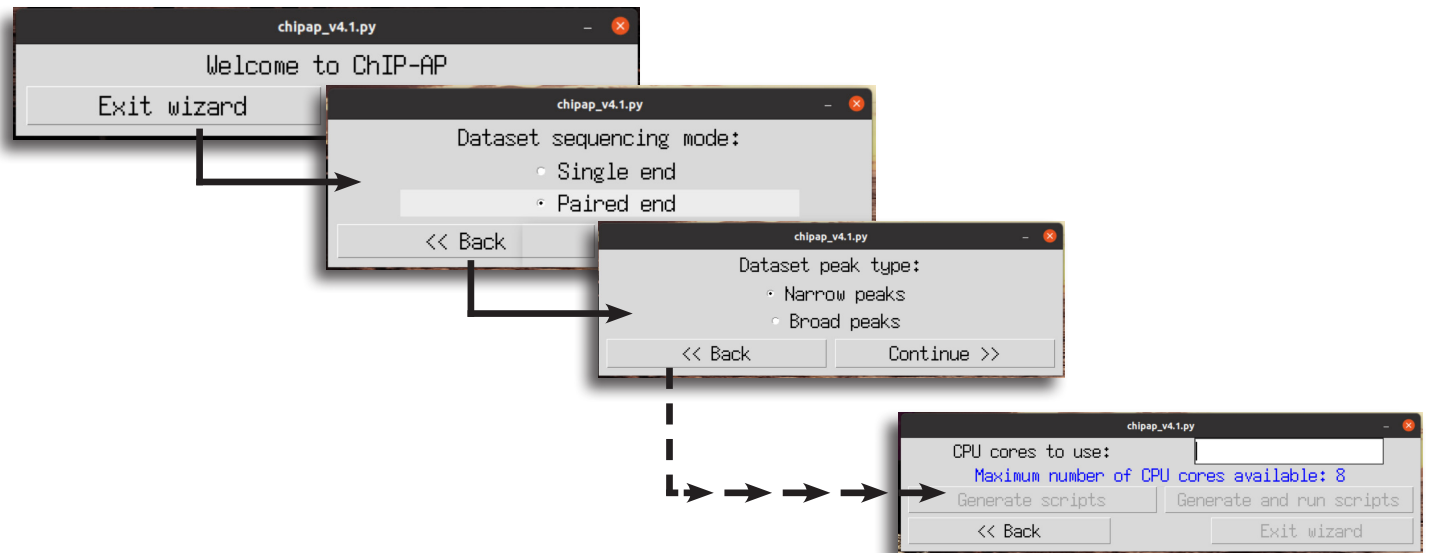
a



b



c



d

